Impact of the Air to Fuel Jet Momentum Ratio on the NO_x Emissions of a Hydrogen Combustion Chamber

Arianna Mastrodonato[1] and Oliver Borm*[1]

[1]Institute for Thermal Turbomachinery and Machine Dynamics, Graz University of Technology, Inffeldgasse 25A, A-8010 Graz, Österreich

Abstract

When considering only hydrogen as fuel the MILD combustion concept provides an interesting opportunity to achieve low NO_x emissions without the need of premixing. Due to the high reactivity of hydrogen, obtaining the desired distributed reaction zone is harder than when using methane as fuel. Thus, it is important to focus on the air to hydrogen jet momentum ratio. This experimental study addresses the NO_x emissions of a hydrogen combustion chamber for different air to fuel jet momentum ratios. Additionally, the chemiluminescence of OH* radicals was measured with an ICCD camera in order to visualise the influence of different fuel inlets onto the reaction zone.

Introduction

The usage of pure hydrogen as fuel in gas turbines avoids the emission of carbon dioxide. If hydrogen is burned with air, the only potential emissions are the oxides of nitrogen (NO_x). Contrary to hydrocarbon fuels, hydrogen has a much higher reactivity. Thus, the lean premixed hydrogen air combustion is afflicted by autoignition and flashback in the premixing zone. Another possibility to achieve low NO_x emissions is the dilution of hydrogen with low oxygen flue gases due to an internal recirculation, which is also known as MILD combustion or flameless oxidation. In order to obtain a MILD combustion regime, a sufficient mixing of fuel and recirculated exhaust gases inside the combustion chamber is required. In a former study Malli et al. [4] identified the importance of the following parameters onto the NO_x emissions of a hydrogen MILD combustion chamber: excess air ratio, thermal power, air momentum as well as air velocity. Changes in the excess air ratio has been accomplished by changing the air or the fuel mass flow. In both investigated cases, the air velocity was kept constant. The evaluation has shown that the NO_x emissions were fairly independent of thermal power for constant excess air ratios, while they increase with increasing excess air ratios when other parameters were kept constant. This can be attributed to the fact that for higher excess air ratios, the oxygen concentration in the recirculated exhaust gases is also increasing. On the other hand, for constant excess air ratio as well as constant air velocity, the NO_x emissions increase slightly with increasing thermal power. Contrary to that, increasing air velocity at constant thermal power and constant excess air ratio reduced the NO_x emissions, due to a stronger recirculation of exhaust gases with lower oxygen concentration.

As it was shown in the preceding study, a flameless oxidation was not possible with that actual geometry. The low fuel momentum was identified as an important influencing parameter. Hence, the aim of the prevailing study is the investigation of the influence of the air to fuel jet momentum ratio onto the NO_x emissions. Additionally, the reaction zone has been visualised with the chemiluminescence of OH* radicals.

*Corresponding author: oliver.borm@tugraz.at

Free Jet Theory

The fuel jet momentum is computed with the help of the continuity equation and ideal gas law:

$$J_{H_2} = \varrho_{H_2} u_{H_2}^2 = \frac{R_{H_2} T_{H_2}}{p_{H_2}} \left(\frac{\dot{m}_{H_2}}{A_{H_2}} \right)^2 \tag{1}$$

In the following discussion, just one hydrogen inlet with a constant area is considered. Staying at the same operating point means approximately constant fuel pressure and temperature. Reducing the number of fuel inlets by two, results in doubling the fuel mass flow but in an increase of fuel jet momentum by a factor of four at one of the remaining inlets, according to Eqn. (2a). The higher fuel jet momentum results furthermore in a higher penetration depth of the fuel jets into the combustion chamber Eqn. (4a).

The same fuel jet momentum can be also achieved by reducing the fuel inlet area, if the number of fuel jets is constant and therefore the fuel mass flow for each inlet is also constant for one operating point. Thus, according to Eqn. (1), in both cases the following proportionality applies for one fuel inlet, assuming an approximately constant density:

$$2\dot{m}_{H_2} \quad \propto \quad 2u_{H_2} \propto 4J_{H_2} \tag{2a}$$

$$\frac{1}{2} A_{H_2} \quad \propto \quad 2u_{H_2} \propto 4J_{H_2} \tag{2b}$$

The assumption of constant fuel density at the same operating point can also be justified, as the fuel Mach number in all cases is well below $Ma_{H_2} < 0.1$, due to the low molecular mass of hydrogen resulting in a very large speed of sound. The influencing parameters of the penetration depth of the round free jet can be estimated in a first approximation by a similarity solution from Schlichting et al. [5, Eq. 12.36]. Hence, the axial

velocity slope at $r = 0$ results in:

$$u_z = \frac{3}{8\pi\mu_{H_2}} \frac{\dot{m}_{H_2} u_{H_2}}{l_z} = \frac{3}{8\pi\mu_{H_2}} \frac{\dot{m}_{H_2}^2}{\varrho_{H_2} A_{H_2} l_z} \tag{3}$$

Considering again the two cases from Eqn. (2) gives the following trend for the penetration depth according to Eqn. (3), measured as that axial position with identical axial velocity, assuming constant viscosity and density:

$$2\dot{m}_{H_2} \propto 4l_z \tag{4a}$$

$$\frac{1}{2} A_{H_2} \propto 2l_z \tag{4b}$$

Thus, even with a constant fuel jet momentum, the penetration depth of one fuel jet is larger for the first case compared to the second case, due to the larger diameter of its inlet. This is also reasonable as in the first case, the number of hydrogen inlets was reduced by two, while in the second case they remain constant. Hence, the overall shear layer of all fuel inlets is larger in case two, which results finally in a shorter penetration depth. Therefore, case one was chosen for the prevailing study, but with the drawback of a more inhomogeneous hydrogen distribution at higher fuel jet momentum. Nevertheless, as can be seen from Eqn. (4) the penetration depth of both cases is larger, compared to the reference case.

Geometry

The hot flow test facility [3, 2] as well as the combustion chamber itself is already described elsewhere [4]. Fig. 1a shows a cut through the liner at the front side with the central air inlet Q and the 16 hydrogen inlets. The liner is rectangular with a length of 330 mm, a width of 130 mm and a height of 240 mm. The optical access has a height of 107 mm and is arranged symmetrically to the air inlet. The optical access starts at the inlet and has a total length of 187 mm. Hence, it doesn't cover the whole length and height of the rectangular liner. Four different configurations with 16, 8,

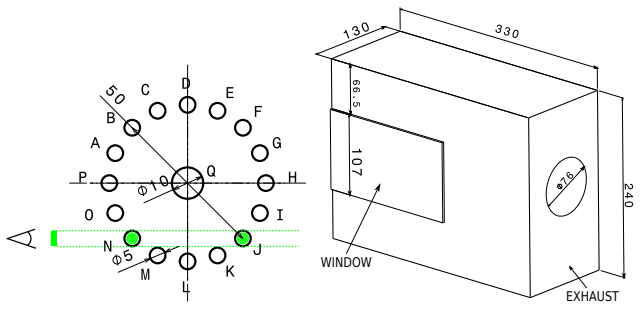

a: Injections at the inlet (upstream view) b: 3D view of the liner

Fig. 1: Geometry

4, and 2 hydrogen inlets have been experimentally investigated. For all the cases except for 16 inlets, some inlets have been closed using criteria of symmetry and uniformity of the flow. Additionally, it was taken into account that there is a roughly 10% higher hydrogen mass flow at inlet D, due to the hydrogen supply system configuration. Furthermore, also the rectangular shape of the liner with higher temperature at the side walls than on the top and bottom walls, as already shown experimentally [4], was considered during the selection of hydrogen inlets. The following inlets have been chosen for the 8 inlets configuration: B, D, F, H, K, L, N, P; for 4 inlets B, F, K, N; and F, N for 2 inlets.

Operating points

The excess air ratio is defined as the actual air–fuel–ratio to the stoichiometric air–fuel–ratio:

$$\lambda = \frac{AFR}{AFR_{st}} \tag{5}$$

Changing the excess air ratio due to different air mass flow at constant thermal power and constant inlet air velocity is only possible if the pressure level would also be changed. As the thermal power has a negligible influence compared to the excess air ratio, it was chosen to have a constant reference pressure and therefore a varying thermal power. The inlet air temperatures correspond to the pressure ratio and an assumed compressor efficiency of about 80%. For each operating point, the cooling air is approximately comparable between the different configurations. The measured air to fuel jet momentum ratios of the air inlet to one fuel inlet are shown in Tab. 2 for the $p_{in} = 6.078$ bar case. As the air momentum is constant for all shown operating points, it can be clearly seen, due to the reduction of the fuel mass flow for one fuel inlet, that the air to fuel jet momentum ratio increases by a factor of four. Thus, the configuration with 16 inlets at λ=2 has the highest momentum ratio, as it has the lowest fuel mass flow in one fuel inlet.

Table 1: Specifications of the different test runs. For the varied parameters, the different values are separated by a semicolon. For all test runs: $v_{air} = 80 \frac{m}{s}$.

run	p_{in} [bar]	T_{air} $[K]$	P_{th} $[kW]$	λ $[-]$
1	2.026	367.0	35.34; 26.50; 21.20	1.2; 1.6; 2.0
2	4.052	463.2	56.01; 42.0; 33.60	1.2; 1.6; 2.0
3	6.078	510.0	76.30; 57.22; 45.78	1.2; 1.6; 2.0

Table 2: Air to Fuel jet momentum ratio for $p_{in} = 6.078$ bar

inlets	$\lambda = 1.2$	$\lambda = 1.6$	$\lambda = 2$
2	50.31	88.63	139.6
4	201.9	357.4	558.8
8	769.9	1436	2279
16	3260	5762	9004

Measurement Techniques

The NO_x emission measurement system [4] as well as the analysis [1] is already described elsewhere. The

OH* radicals were detected with an ICCD camera (NanoStar, 1280x1024 pixel) together with an UV lens (105 mm, aperture: f/4.5, Nikon) and processed with the DaVis software from LaVision. Additionally, a TECHSPEC band–pass filter at 310 nm was used (310±3 nm CWL, FWHM 10±2nm bandwidth, 50 mm mounted diameter, 18% transmission, Edmund Optics). The images were captured with the following parameters, which were held constant for all operating points: delay: 0.1, burst count: 100, decay: 100, gain: 35. The position of the ICCD camera is marked as an eye in Fig. 1a. As the absorption of the gas is negligible, the camera detects all OH* emissions along the line of sight for each pixel. Thus, the emission of OH* radicals in the top and bottom of the fuel injection annulus might be overpredicted, since the OH* emissions from two or more fuel jets are integrated. For each operating point 200 images have been taken at a frequency of 1 Hz. During the post processing, these images have been averaged with the software and from the resulting image, a reference image has been subtracted in order to strip any other OH* emission independent from the combustion. The reference image, without combustion, has been obtained with an average of 60 images, captured as before. As the camera has a 12 bit depth the images were finally exported with an identical colour scale of 4096 counts.

NO_x Emissions

The NO_x emissions were corrected to a reference oxygen concentration of 15 Vol.-% in order to compare them quantitatively. For all four configurations, three operating points for each reference pressure were investigated experimentally, varying the excess air ratio by varying the thermal power at constant air mass flow as well as constant pressure level according to Tab. 1. For all pressure levels it can be shown that the lowest NO_x emissions can be achieved with lower excess air ratio. Hence, the influence of the lower oxygen concentration in the recirculated flue gas is clearly observable. The slopes of the configurations with 4, 8 and 16 fuel inlets are similar, while the 2 inlet configuration has a steeper slope for all pressure levels. Due to this different slope, the corrected NO_x emissions of the 2 inlet configuration are at λ=1.2 always comparable to the 4 inlet configuration. While at λ=2, the 2 inlets have a distinct higher NO_x emission than the other three configurations. Furthermore, the NO_x emissions of the 8 and 16 inlets configurations are similar in all cases, with always slightly lower NO_x emission for the 8 inlets. This might be attributed to the fact that the fuel jet momentum of the 8 inlets is four times higher than the 16 inlets configuration, but the overall reacting flow field is still comparable between these two configurations. An additional increase of the fuel jet momentum by reducing the fuel inlets to 4, results in a further reduction of the corrected NO_x emissions. The influence of the higher fuel jet momentum is more pronounced with increasing pressure level, while at a lower pressure of 2 bar the difference between the 4, 8 and 16 inlets is not so distinct. Thus, at constant internal aerodynamics, such as constant inlet velocities, inlet temperatures and pressures, the corrected NO_x emissions decrease with a decreasing excess air ratio, even if this results in an increase of thermal power.

In Fig. 5 the corrected NO_x emissions are shown as a

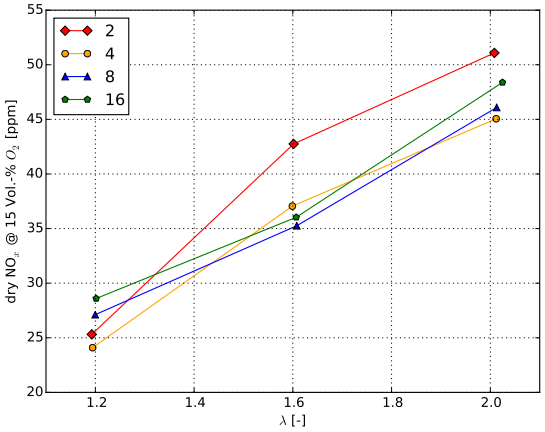

Fig. 2: Corrected NO_x emissions; p_{in}=2.026 bar

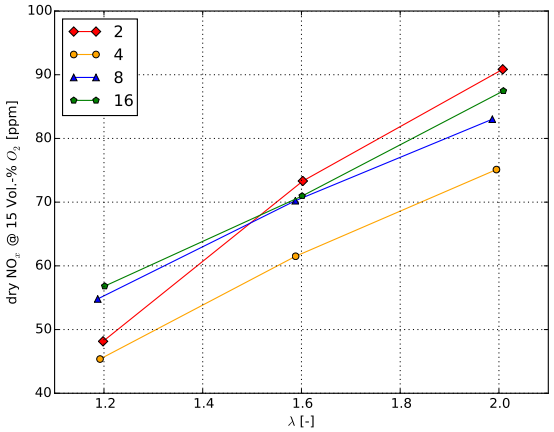

Fig. 3: Corrected NO_x emissions; p_{in}=4.052 bar

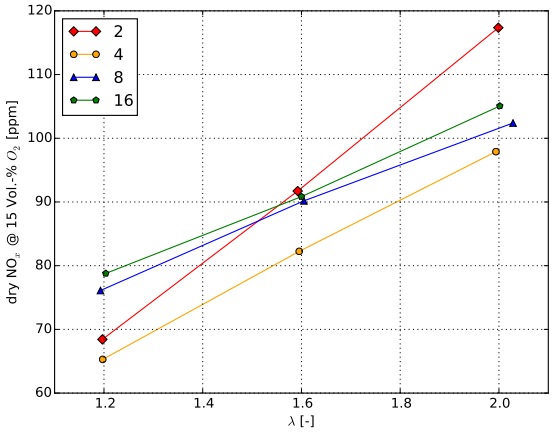

Fig. 4: Corrected NO_x emissions; p_{in}=6.078 bar

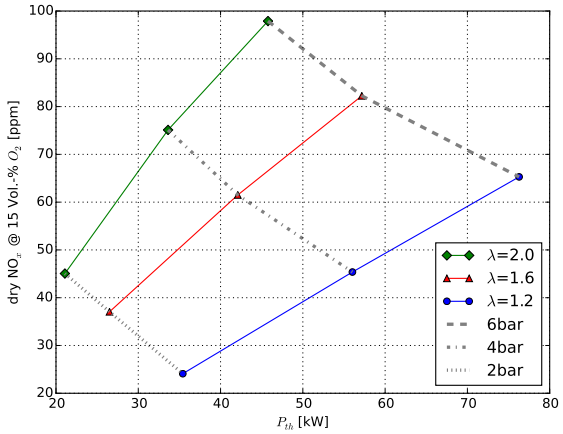

Fig. 5: Corrected NO_x emissions; 4 inlets

function of thermal power for the 4 inlets configuration. At a constant reference pressure, again, the main influencing parameter is the excess air ratio. Contrary to that, for constant excess air ratios, the corrected NO_x emissions are increasing with thermal power. The air inlet temperature was changed for each reference pressure according to Tab. 1. Thus, that influence onto the corrected NO_x emissions was not yet evaluated independently.

Chemiluminescence of OH* radicals

The influence of the jet momentum onto the shape of the reaction zone can be investigated qualitatively by the measurement of OH* radicals. It is assumed in general that the shape of the reaction zone as well as the intensity of the OH* emission are proportional to the heat release rate. Furthermore, if the volume of the heat release remains the same, the temperature rise is also proportional to the heat release rate. For hydrogen air combustion, the oxides of nitrogen are mainly produced as thermal NO_x. Therefore, a relatively long residence time as well as high temperatures are required. As the internal aerodynamics of the combustion chamber in the actual experiments was not changed, it is assumed that the residence time is comparable for all cases. Hence, the main influence on the NO_x production will be the locally different temperatures, which can be associated in a first glance to the intensity of the OH* emissions with the given assumptions. As previously shown (c.f. Tab. 2) the air to fuel jet momentum ratio is lower for lower excess air ratio as the thermal power increases. To show the influence of the excess air ratio onto the reaction zone, operating points with λ=1.2 and 2 have been chosen.

Due to the low fuel jet momentum at λ=2 the configurations with 4, 8 and 16 inlets show their highest OH* emissions in the shear layer of the air jet (Fig. 6). Additionally, these peaks are directly near the air inlet. Nevertheless, the measurement of the OH* emissions is a linear projection from the 3D reaction zone onto a 2D plane. Thus, the OH* radicals on top and bottom of the shear layer annulus are overpredicted for these configurations, due to the measurement along the line of sight as already shown in Fig. 1a. The reaction zone for the 2 fuel inlets configuration looks differently, mainly due to the higher fuel momentum. This configuration does not have any OH* emission in the shear layer of the air jet. Furthermore, the inhomogeneity of the two discrete inlets is more pronounced in the chemiluminescence images. Even if the projected emission of OH* radicals are lower than the 4 inlets configuration, the heat release rate maybe locally higher for 2 inlets due to the larger inhomogeneity, resulting in higher peak temperatures and thus, higher NO_x emissions.

Also at λ=1.2 the highest OH* emission can be found in the shear layer of the air jet for 4, 8 and 16 inlets (Fig. 7). For the case with 16 inlets, the peak can be found again directly near the air inlet. Thus, a dilution of hydrogen with recirculated flue gas is barely impossible before the combustion. For 8 and 4 fuel inlets the main reaction zone also corresponds to the air shear layer. Additionally, the OH* emissions are again overpredicted at the top and bottom of that shear layer. Again the reaction zones for 4, 8 and 16 inlets are comparable. Thus, these shapes explain the similar slopes of the NO_x emissions for all cases, contrary to the 2 inlets configuration. The reaction zone of the 2 inlets is again shifted in radial direction and once again not coincident with the shear layer of the air jet.

The oxygen concentration of the recirculated flue gas is higher considering λ=2 (Fig. 6) compared to λ=1.2 (Fig. 7). Hence, at λ=1.2 the reaction zone is stretched more downstream than at λ=2 for all configurations. Nevertheless, for 4, 8 and 16 inlets the highest OH* emissions can be found for both excess air levels in the shear layer of the air jet. Therefore, a dilution of hydrogen with flue gas is rarely possible. Due to the higher fuel jet momentum at 2 inlets, the peaks of OH* emissions are neither present in the shear layer nor in the inlet cone of the round air jet, as can be clearly seen in Fig. 7a. Hence, the dilution of the fuel jet with recirculated exhaust gas is much better, compared to the other configurations at λ=1.2. This has a more pronounced effect in the reduction of NO_x emissions. On the other side, this configuration, with only two inlets, leads to a higher inhomogeneity, and this creates a large drawback in NO_x emissions at λ=2, due to the higher oxygen concentration. As can be seen in Fig. 6a the heat release is much higher near the fuel inlet than in Fig. 7a, due to the much better dilution in the latter case. Thus, the advantage of a higher fuel momentum at 2 inlets, due to a higher dilution, has at the same time the drawback of a higher inhomogeneity. The influence of the oxygen concentration is for the 2 inlet configuration more pronounced due to the larger inhomogeneity of the fuel injection. This results finally in a steeper slope of the NO_x emissions as can be seen in Fig. 4.

Conclusion

Within this study, a hydrogen combustion chamber was investigated experimentally at three different pressure levels. The air jet momentum was held constant for all operating points of one reference pressures. The

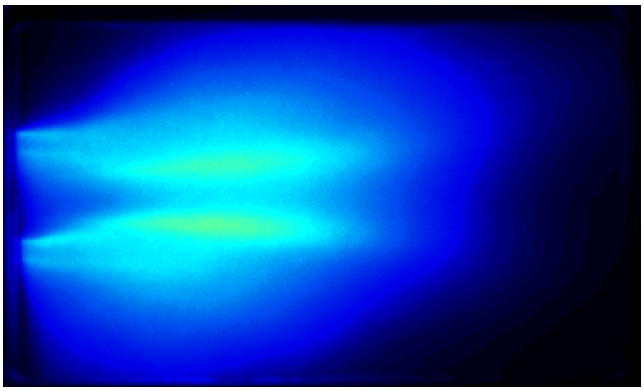

a: 2 inlets

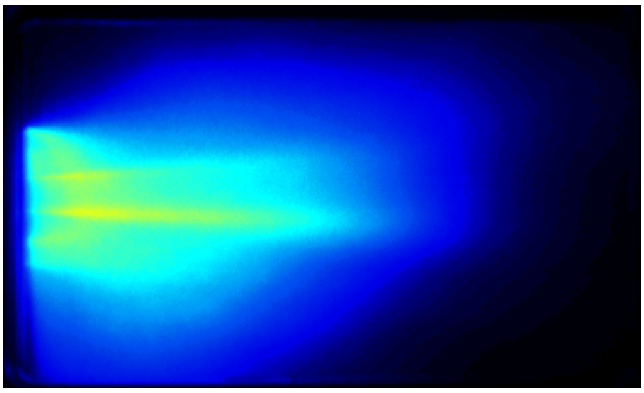

b: 4 inlets

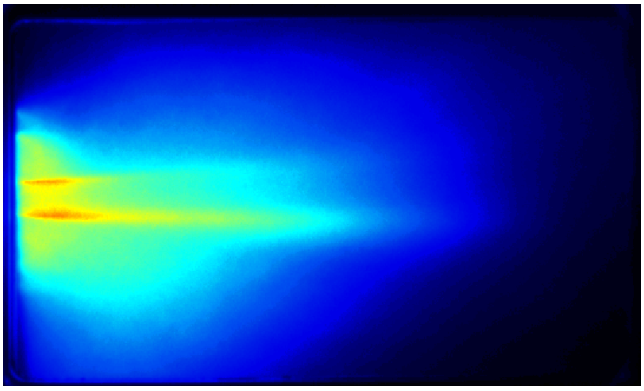

c: 8 inlets

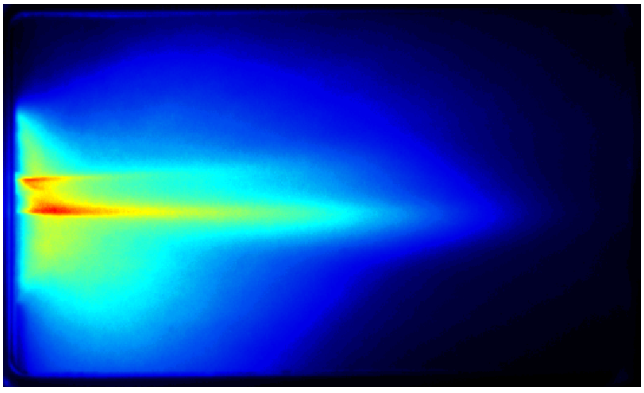

d: 16 inlets

Fig. 6: λ=2, p_{in}=6.078 bar, P_{th}=45.78 kW

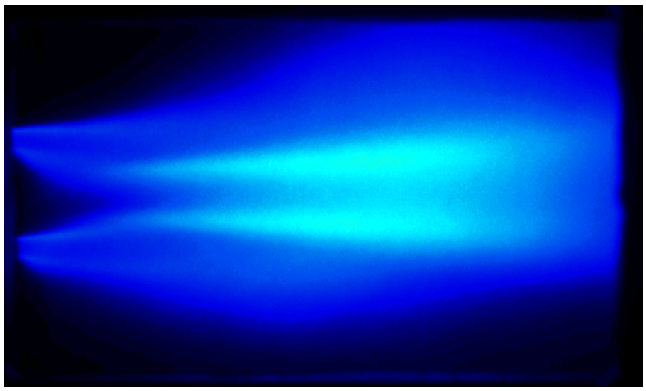

a: 2 inlets

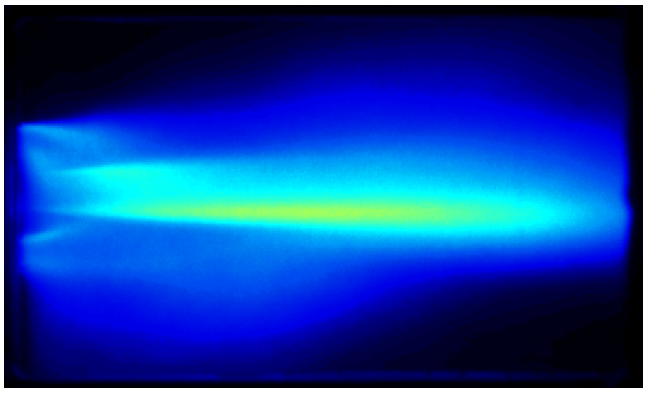

b: 4 inlets

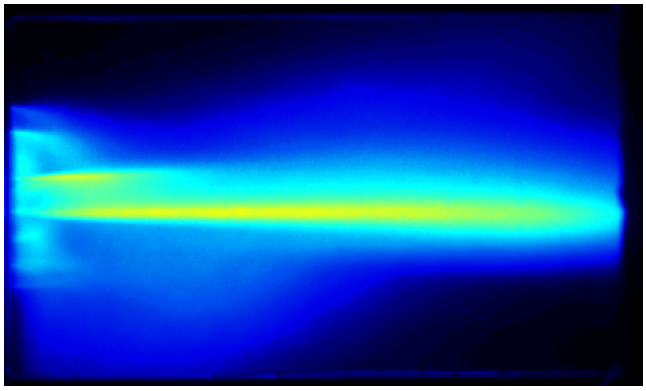

c: 8 inlets

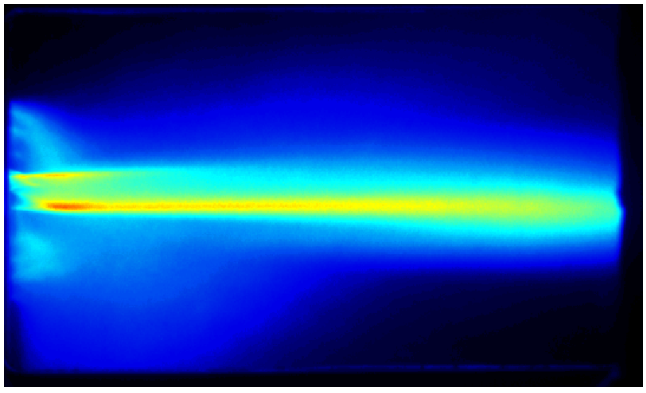

d: 16 inlets

Fig. 7: λ=1.2, p_{in}=6.078 bar, P_{th}=76.30 kW

number of fuel inlets was successively reduced, resulting in a continuous increase of fuel jet momentum in the remaining fuel inlets. The injection at higher fuel momentum has the drawback of a larger fuel inhomogeneity. For all investigated configurations, higher excess air ratios, which also mean higher oxygen concentrations, result in higher NO_x emissions. Reducing the air to fuel jet momentum ratio reduces also the NO_x emissions as long as the reaction zones have a similar shape. Due to the high fuel momentum at 2 inlets, the reaction zone is different. The results have also shown that the influence of oxygen concentration is strongly dependent on the homogeneity of the fuel injection. For the actual investigated cases, lower air to fuel jet momentum ratio results in a higher inhomogeneity of the flow. At the same time a lower air to fuel jet momentum ratio, which means higher fuel jet momentum in the actual cases, eventually results in a better dilution of the fuel with the recirculated exhaust gases, leading to lower NO_x emissions at low excess air ratios.

In order to quantify the influence of the fuel jet momentum separately to the fuel inhomogeneity, further experiments are necessary. Increasing the fuel jet momentum at a more homogeneous flow can be accomplished by reducing the fuel inlet diameter while maintaining the number of hydrogen inlets. Additionally, the influence of the inlet air temperature onto the NO_x emissions has to be investigated independently of the pressure level. A 3D CFD calculation with an appropriate turbulent chemistry model, like the Eddy Dissipation Concept (EDC), would assist the further understanding of the turbulent reacting flow field.

Acknowledgements

This work was financed by the national project 'Hy4JetEngines' as part of the 'Austrian Aeronautics Programme TAKE OFF' of the Austrian Research Promotion Agency (FFG). Special thanks goes to Johannes Peterleithner and Jakob Woisetschläger who contributed essentially to the set up of the chemiluminescence system.

Nomenclature

A	injection area
AFR	air mass flow to fuel mass flow
J	momentum
l_z	penetration depth
λ	excess air ratio
$\dot{m}$	mass flow
Ma	Mach number
NO_x	oxides of nitrogen
p	pressure
P_{th}	thermal power
ϱ	density
R	specific gas constant
T	temperature
u	velocity

References

[1] Borm, O. : Evaluation of gaseous emissions from hydrogen combustion aircraft engines. In: *Proceedings of ASME Turbo Expo 2014, Düsseldorf, Germany*, 2014. – GT2014-25470

[2] Leitgeb, T. ; Giuliani, F. ; Heitmeir, F. : Design And Adaptiation of The Air System For A Versatile Turbine And Combustion Chamber Test Facility. In: *Proceedings of 8th European Conference on Turbomachinery, Graz*, 2009, S. 853 – 863

[3] Leitgeb, T. ; Giuliani, F. ; Niederhammer, A. ; Pirker, H.-P. : Computer Aided Dimensioning And Validation of A Versatile Test Facility For Combustion Chambers And Turbines. In: *Proceedings of ASME Turbo Expo 2009, Orlando, USA*, 2009. – GT2009-59592

[4] Malli, H. ; Eckerstorfer, K. ; Borm, O. ; Leitl, P. : Experimental and Numerical Investigation of a Hydrogen Combustion Chamber under various Inlet Conditions. In: *Proceedings of ASME Turbo Expo 2014, Düsseldorf, Germany*, 2014. – GT2014-25472

[5] Schlichting, H. ; Gersten, K. : *Grenzschicht-Theorie*. 10. Springer, 2006